Silicon-Nitride-based Passive Photonic Platform for Visible and Telecommunications Wavelength Regions

Yuriko Maegami, Guangwei Cong, Morifumi Ohno, Toshihiro Narushima, Noritsugu Yamamoto, Hitoshi Kawashima and Koji Yamada
National Institute of Advanced Industrial Science and Technology (AIST)
16-1 Onogawa, Tsukuba, Ibaraki, 305-8569, Japan
E-mail: yuriko-maegami@aist.go.jp

***Abstract*—We confirmed a wide band visible light transmission in waveguides utilizing silicon nitride films deposited by CMOS compatible CVD, and also observed a reversible refractive index change of the films in a 1300-nm wavelength band.**

Keywords—silicon nitride, CMOS compatible, visible waveguide, reversible refractive index change, dangling bonds.

I. Introduction

Photonic integrated circuits (PICs) with complementary metal-oxide semiconductor (CMOS) compatible process paves the way for not only telecommunications applications but also sensing, neural network and quantum information [1-3]. A silicon nitride (SiN) film is attractive attention for a highly-CMOS compatible material, which is generally deposited by plasma-enhanced chemical vapor deposition (PECVD) or low-pressure chemical vapor deposition (LPCVD). The refractive index of the SiN can be typically tuned 1.9–2.0. Therefore, the core of a SiN waveguide reaches around a micrometer in the telecommunications band, and thus the fabrication tolerance can also be relaxed compared to silicon waveguides. For visible light, that still stays sub-micrometers levels, and thus standard CMOS fabrication process can be applied to building waveguide structures.

In this work, as a promising application of these CMOS compatible silicon nitride films to an integrated photonic platform, we demonstrate a visible light transmission in a LPCVD-SiN-based waveguide and evaluated its absorption loss and scattering loss. Moreover, we observe a reversible refractive index change of a PECVD-SiN film in the telecommunications band by alternately processing of the thermal annealing and ultraviolet (UV) irradiation.

II. CMOS Compatible SiN Films

Two SiN films were formed by different types of film deposition methods. One was deposited by a PECVD at a relatively low temperature of 170 ℃ using SiH_4 and NH_3. Another was deposited by a LPCVD at a high temperature of 760 ℃ using H_2SiCl_2 and NH_3. At first, we examined the material characteristics of our PECVD- and LPCVD-SiN films. Average atomic composition of the films, quantitatively measured by Rutherford backscattering spectrometry, were 3:3.8 and 3:4.1 for the PECVD- and LPCVD-SiN films, respectively. We confirmed that the PECVD-SiN film is nonstoichiometric and has a Si-rich composition, while the LPCVD-SiN film is almost stoichiometric. Next, we examined the optical properties of refractive index and extinction coefficient. Figure 1 shows extinction coefficients of PECVD- and LPCVD-SiN films in an UV region. The increase of extinction coefficient of PECVD-SiN film can be seen in a longer wavelength region compared with that of LPCVD-SiN film. The result suggests that the bandgap of PECVD-SiN is narrower than that of LPCVD, and the PECVD-SiN would not be suitable for visible light transmission.

III. SiN Waveguide for Visible Light

At visible light wavelengths, the LPCVD-SiN film is transparent, and the SiN based PICs are in demand for applications such as biosensing and quantum information, etc. However, the SiN waveguide has a large refractive index contrast between core and clad, and the optical field is tightly confined in the core of the waveguide. Therefore, scattering losses would become large. To reduce propagation loss of waveguides, it is very important for us to know the contribution of scattering loss and material absorption in a total propagation loss. However, a measurement limit of optical properties in conventional measurement methods, such as a spectroscopic ellipsometry and an interference spectrophotometry, is too large to be applied to the evaluation of waveguide propagation. For example, typical measurement limit of extinction coefficient is around a 10^{-4}, which corresponds to a very large propagation loss of around a hundred dB/cm. For the more accurate evaluation of material absorption, we made use of the difference of propagation losses for different waveguide structures, such as thicknesses and widths [4]. The thicknesses of the waveguide were 80 and 200 nm, and for each thickness, the widths were set to 300 to 600 nm. Figure 2 shows the propagation loss of the SiN waveguide with respect to the core width at the wavelength of 452 nm and 524 nm, respectively. The polarization was set to the quasi-TE mode. The bending loss of the 100-μm radius

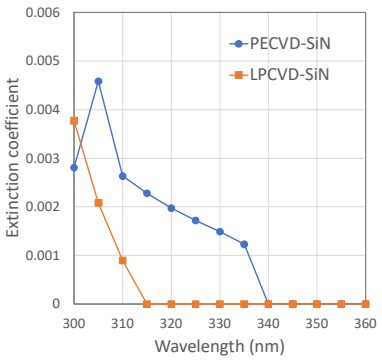

Fig. 1 Extinction coefficient of the as-deposition PECVD- and LPCVD-SiN films in the UV region.

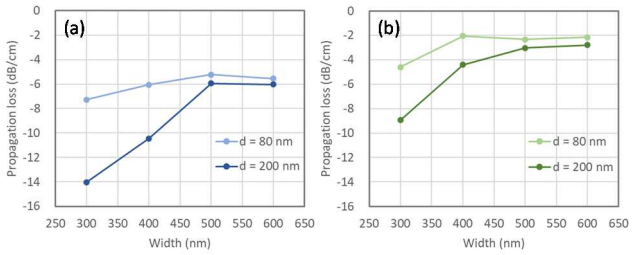

Fig. 2 Propagation loss of the SiN waveguide with respect to the core width at the wavelength of (a) 452 nm and (b) 524 nm.

can be negligible. The propagation loss became lower with increasing width and shows almost no change regardless of the core dimension above the width of 500 nm. Although we didn't show here, transmission loss for 634 nm wavelength was lower than those for 452/524 nm wavelength. Since the scattering loss is proportional to the reciprocal of the fourth power of the width [5], it is considered the scattering loss reaches negligible levels. The propagation loss almost corresponds to the absorption loss, which can be expressed as $\alpha = \alpha_{SiN} \times \tau + \alpha_{SiO2} \times (1 - \tau)$, where α_{SiN} and α_{SiO2} is material absorption loss of SiN core and SiO_2 clad, τ is the confinement factor of SiN core. Table 1 summarizes the material absorption loss of SiN and SiO_2 at the core width of 600 nm for each wavelength. These losses correspond to an extinction coefficient on the order of 10^{-6}, which is far below the analytical limit (10^{-4}) of spectral ellipsometry. We can also estimate the scattering loss by subtracting the absorption loss from the propagation loss. Thus, the scattering loss is largest with the 300 nm-wide and 200 nm-high core, which is 8.1 dB/cm and 6.3 dB/cm at the wavelength of 452 nm and 524 nm, respectively.

TABLE I. MATERIAL ABSORPTION LOSS OF SIN AND SIO2

	452 nm	524 nm
α_{SiN}	6.1 dB/cm	2.9 dB/cm
α_{SiO2}	4.6 dB/cm	1.4 dB/cm

IV. REVIERSIBLE REFRACTIVE INDEX CHANGE OF SIN FILM

Photonic neural network and photonic quantum operation using PICs are paid attention as next generation computing systems with low-latency and high-throughput photonic processing accelerators. These consist of a lot of waveguide-based interference devices whose phase control is generally used micro-heaters based a thermo-optic effect. Therefore, the large electric power consumption to keep circuit parameters is critical issue and non-volatile interference circuits which don't require any electric power are demanded.

The PECVD- and LPCVD-SiN films are the highly-CMOS compatible material, which contain Si and N dangling bonds. Electronic charge states of the dangling bonds can be converted by the UV irradiation and annealing at 200-300 ℃ [6, 7]. The UV light irradiation causes the state transition of K-center attributed to Si dangling bonds from K+/- to K^0 while the annealing causes the state transition from K^0 to K+/-. This reversible state transition is accompanied with a change of absorption coefficient in visible-UV wavelength region [8]. Considering Kramers-Kronig relation, it is natural that this transition is also accompanied with a refractive index change in telecommunication wavelength band around 1300 nm, and the transition would have potential for non-volatile photonic interference circuits.

To experimentally confirm the refractive index change in telecommunication wavelength band, we alternately processed the annealing and UV irradiation to the SiN films [9]. The annealing was performed at 300 ℃ on a hot plate for 30 minutes under an atmospheric condition. The UV irradiation was also performed for 30 minutes without an ozone generation by using an UV ozone cleaner (UV-1 developed by Samco Inc.). The UV illuminance is about 40 mW/cm^2 at the wavelength of 254 nm. The measurement samples were pretreated by repeating the annealing and UV irradiation more than 4 times. By using ellipsometry measurement and analysis (J. A. Woollam visible-angle spectroscopy ellipsometer (VASE)) at the wavelength from 300 to 2500 nm, we evaluated the refractive index and extinction coefficient after each processing of the annealing and UV irradiation.

Figure 3(a) shows the spectral extinction coefficient of the PECVD- and LPCVD-SiN at the wavelength range from 300 to 340 nm. In the PECVD-SiN film, the spectra of UV irradiation are clearly separated from that of annealing. On the other hand, in the LPCVD-SiN film, the spectral difference between the UV irradiation and annealing are very slight. Figure 3(b) shows the extinction coefficient, averaged in these wavelength range. The PECVD-SiN exhibits an apparent reversible change of extinction coefficient with respect to the alternately the annealing and UV irradiation. The amplitude of the extinction coefficient change in the PECVD-SiN was 0.0013, which was 17 times larger than that in the LPCVD-SiN. The reversible extinction coefficient change in the

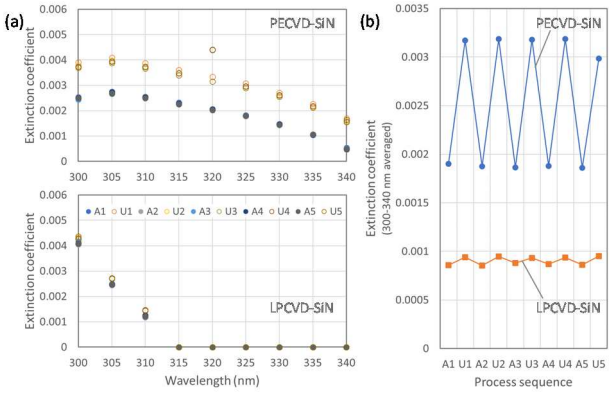

Fig. 3 (a) Spectral extinction coefficient and (b) averaged extinction coefficients of the PECVD- and LPCED-SiN films in 300-340 nm wavelength band andIn horizontal axis, "A" and "U" mean the processing of the annealing and UV irradiation, respectively.

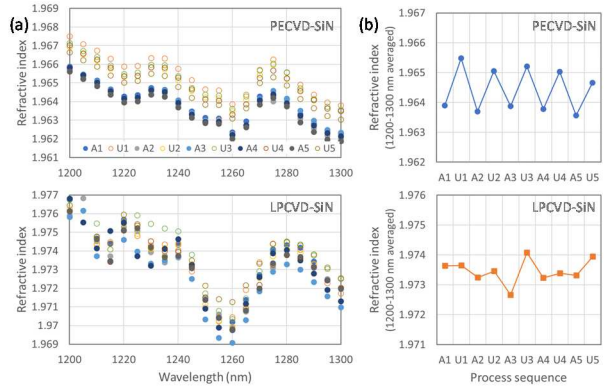

Fig. 4 (a) Spectral refractive index and (b) averaged refractive indices of the PECVD- and LPCED-SiN films in 1200-1300 nm wavelength band.

PECVD-SiN seems to be the same phenomena as those due to the state transition of K-centers reported in [8].

Figure 4(a) shows the spectral refractive index of the PECVD- and LPCVD-SiN at the wavelength range from 1200 to 1300 nm, which is often used for telecommunication applications. In the PECVD-SiN film, the spectra were divided into the UV irradiation and annealing groups. On the other hand, in the LPCVD-SiN film, we cannot distinguish the spectra of the UV irradiation and annealing. Figure 4(b) shows the refractive index averaged in theses wavelength range. The PECVD-SiN exhibits an apparent reversible change of the refractive index, while the LPCVD-SiN exhibits no apparent change. The amplitude of refractive index change in the PECVD-SiN is about 0.0014 averaged through the whole process sequence.

The zigzag behavior of the refractive index corresponds to that of the extinction coefficient, and thus would be originated in the state transition of K centers. Electron spin resonance (ESR) measurements of these materials after UV irradiation have given a K^0 spin density of over 5×10^{18} cm^{-3} for PECVD-SiN and less than 1×10^{18} cm^{-3} for LPCVD one. Since the PECVD-SiN has a silicon rich composition and include much more K-centers than the LPCVD one, the refractive index change can have been clearly observed. The obtained amplitude of refractive index change is sufficient for constructing non-volatile PICs.

V. Summary

We confirm a wide band visible light transmission waveguides utilizing SiN films deposited by LPCVD. From the propagation property of the waveguide, we discriminated material absorptions and scattering loss from total propagation loss. The evaluation process would be very useful in designing SiN waveguide devices in visible region. The Moreover, we observed a reversible refractive index change of PECVD-SiN film by alternately processing of the annealing and UV irradiation in the telecommunications band and found a potential to be applicable to non-volatile photonic interference circuits.

Acknowledgment

The authors thank all staffs at the TIA-SCR station for device fabrication.

References

[1] Euijae Shim, Yu Chen, Sotiris Masmanidis, and Mo Li, "Multisite silicon neural probes with integrated silicon nitride waveguides and gratings for optogenetic applications," Sci. Rep., vol. 6, 22693 pp. 1–5, March 2016.

[2] Guangwei Cong, Noritsugu Yamamoto, Takashi Inoue, Yuriko Maegami, Morifumi Ohno, Shota Kita, Shu Namiki, and Koji Yamada, "On-chip bacterial foraging training in silicon photonic circuits for projection-enabled nonlinear classification," Nat. Commun., vol. 13, 3261 pp. 1–12, June 2022.

[3] G. Zhang, J. Y. Haw, H. Cai, F. Xu, S. M. Assad, J. F. Fitzsimons, X. Zhou, Y. Zhang, S. Yu, J. Wu, W. Ser, L. C. Kwek, and A. Q. Liu, "An integrated silicon photonic chip platform for continuous-variable quantum key distribution," Nat. Photonics, vol. 13, pp. 839–842, August 2019.

[4] Yuriko Maegami, Makoto Okano, Guangwei Cong, Keijiro Suzuki, Morifumi Ohno, Toshihiro Narushima, Nobuyuki Yokoyama, Miyoshi Seki, Shigeru Saitou, Minoru Ohtsuka, Hitoshi Kawashima, and Koji Yamada, "CMOS-Compatible Silicon Nitride Waveguide on Silicon Photonics Platform," OSA Advanced Photonics Congress 2021, paper ITu3A.3, July 2021.

[5] F. P. Payne, and J. P. Lacey, "A theoretical analysis of scattering loss from planar optical waveguides," Opt. Quantum. Electron. vol. 26(10), pp. 977–986, October 1994.

[6] W.L. Warren, J. Robertson, and J. Kanicki, "Si and N dangling bond creation in silicon nitride thin films," App. Phys. Lett. vol. 63, pp. 2685–2687, November 1993.

[7] D. Chen, J.M. Viner, P.C. Taylor, and J. Kanicki, "Photoluminescence and electron spin resonance in nitrogen-rich amorphous silicon nitride," J. Non-Cryst. Solids. vol. 182, pp. 103–108, March 1995.

[8] K. Kanicki, and W.L. Warren, "Defects in amorphous hydrogenated silicon nitride films," J. Non-Cryst. Solids, vol. 164-166, pp. 1055–1060, December 1993.

[9] Yuriko Maegami, Gangwei Cong, Morifumi Ohno, Toshihiro Narushima, Noritsugu Yamamoto, Hitoshi Kawashima, and Koji Yamada, "Observation of Reversible Refractive Index Change of CMOS-Compatible Silicon Nitride Film," 2022 International Conference on Solid State Devices and Materials, A-9-05, Sptember 2022.